

Engineering Aspects of Enzymatic Signal Transduction: Photoreceptors in the Retina

Peter B. Detwiler,* Sharad Ramanathan,[†] Anirvan Sengupta,[†] and Boris I. Shraiman[†]

*Department of Physiology and Biophysics, University of Washington, Seattle, Washington 98195 and [†]Bell Laboratories, Lucent Technologies, Murray Hill, New Jersey 07974 USA

ABSTRACT Identifying the basic module of enzymatic amplification as an irreversible cycle of messenger activation/deactivation by a “push-pull” pair of opposing enzymes, we analyze it in terms of gain, bandwidth, noise, and power consumption. The enzymatic signal transduction cascade is viewed as an information channel, the design of which is governed by the statistical properties of the input and the noise and dynamic range constraints of the output. With the example of vertebrate phototransduction cascade we demonstrate that all of the relevant engineering parameters are controlled by enzyme concentrations and, from functional considerations, derive bounds on the required protein numbers. Conversely, the ability of enzymatic networks to change their response characteristics by varying only the abundance of different enzymes illustrates how functional diversity may be built from nearly conserved molecular components.

INTRODUCTION

One of the requirements of life at the single-cell or multicellular level is the ability to detect external stimuli and convert them into biologically meaningful intracellular signals. Such events underlie unicellular chemotaxis, sensory reception by specialized cells, and the intercellular communications that are necessary for the development and functioning of multicellular animals. In the majority of these cases, the external signal is a molecular ligand that, by binding to a specific membrane receptor protein, triggers a cascade of enzymatic reactions that ultimately lead to the activation of an effector. The resulting cellular response is capable of adapting to the level of the external signal and may be contingent on the presence or absence of other signals (Koshland, 1980; Gerhart and Kirschner, 1997). Enzymatic signal transduction pathways are characteristically heavily regulated through feedback and multiple modulators. The control of gene expression, for example, typically involves the integration of many signals and employs complex enzymatic networks, which effectively implement logical functions (Bray, 1995; Wray, 1998; Ptashne, 1992). In contrast, olfaction and photoreception involve simpler enzymatic cascades which may be thought of as adaptive amplifiers or transducers (Reed, 1990; Stryer, 1991; Koshland, 1980) that detect an extracellular stimulus and convert it into an intracellular signal that can effectively control the information content of the cellular output signal, i.e., neurotransmitter release. Photoreceptors—the rod and cone cells of the retina—are unique because instead of molecular ligands they transduce a particularly potent input,

the visible light quanta, which carry ~ 50 kcal of energy. However, downstream from the specially adapted 7-helix transmembrane receptor protein, rhodopsin, the enzymatic cascade responsible for phototransduction employs molecular elements that are ubiquitous and standard components in biological signaling pathways. These include a heterotrimeric G-protein (transducin) (Alberts et al., 1994; Stryer, 1995; Simon et al., 1991), an effector enzyme (phosphodiesterase, PDE), and intracellular signals that are carried by changes in a cyclic nucleotide (cGMP) and Ca. In addition, the components of this cascade are organized in a way that is similar to many other chemical signal transduction pathways. Below we shall take advantage of the great deal of knowledge of the electrophysiology and biochemistry of rods and cones and use photoreceptors as a case study in our discussion of the general engineering principles of signal transduction.

Modern genetic and biochemistry methods have led to the discovery of a multitude of signaling cascades. The identification of the molecular elements and their interactions has provided detailed information about “how” a wide variety of specific pathways work. But little attention has been given to considering broader questions about the general system-level properties of signaling cascades and “why” they are designed the way they are. Such an approach might start with the formulation of the engineering requirements and the physical constraints on signal transduction and, by identifying common biochemical modules and their regulatory motifs, demonstrate how these functional requirements are met. The ultimate goal is to provide a unified view of the comparative physiology and biochemistry of signal transduction in the context of evolution (Gerhart and Kirschner, 1997) and to give quantitative insight into the regulatory mechanisms and the system-level consequences of the modulation/modification of the components.

Below, with the example of vertebrate phototransduction in mind, we shall examine an enzymatic cascade in general engineering terms. Following Stadman (Stadman and

Received for publication 2 November 1999 and in final form 5 September 2000.

Address reprint requests to Dr. Boris I. Shraiman, Bell Labs, Lucent Technologies, Room 1D-236, 700 Mountain Avenue, Murray Hill, NJ 07974. Tel.: 908-582-2968; Fax: 908-582-4702; E-mail: boris@physics.bell-labs.com.

© 2000 by the Biophysical Society

0006-3495/00/12/2801/17 \$2.00

Chock, 1977; Chock and Stadman, 1977) and Koshland (Koshland et al., 1978), we identify the amplifier modules of the cascade as irreversible messenger activation loops with “push-pull” control by opposing enzymes. We then characterize this enzymatic amplifier in terms of the engineering parameters such as gain, bandwidth (i.e., inverse characteristic time of the response), and noise and demonstrate how these parameters may be “tuned” by adjusting enzyme concentrations. We will make clear the competition between the gain and bandwidth and the relation between the noise (due to fluctuations in reactions), bandwidth, and dissipated power. These are the engineering characteristics that determine the rate of information transfer in the signal transduction channel, and we provide the information theoretic considerations which govern the optimization of the design of the cascade; e.g., we determine the gain requirements and the optimal input/output relation. We shall also discuss the role of adaptation, which corresponds to a slow change in the optimal input/output mapping in response to a change in the statistical properties of the input.

With the framework of the engineering description in place, one can inquire how a cell controls the basic parameters of its transduction pathway. In the past, much of the discussion of enzymatic cascades has focused on the often remarkable properties of its molecular components (e.g., the impressive catalytic efficiency of phosphodiesterase; Stryer, 1995). Yet the time scale for protein evolution is slow, and the relevant engineering parameters of the transduction system would be more readily modified through the adjustment of molecular concentrations rather than their kinetic constants. We shall explicitly identify the parametric dependence of the engineering characteristics of the phototransduction cascade on the concentration of its key protein elements. This has allowed us to obtain bounds on the minimal amount of enzymes required to achieve the observed functional performance of rods which are consistent with prior measurements and to identify different means of controlling and regulating their performance characteristics.

In the next section, a generic enzymatic amplifier unit is described and analyzed in terms of gain, bandwidth, and power dissipation. The following section presents a general treatment of noise in the enzymatic amplifier. The section, Enzymatic Cascade, deals with general properties of amplifier cascades, and the following section discusses and parameterizes the effect of feedback. The section, Minimal Required Gain and Minimal Messenger Concentration, shows how the signal-to-noise considerations lead to a minimal gain requirement and to a bound on the necessary amount of transduction messenger molecules. The section, Optimization of Input/Output Relation and Adaptation, outlines the information theoretic considerations governing the design of the signal transduction system and discusses optimization and adaptation. Enzymatic Amplifier Cascade in Phototransduction analyzes the organization of the vertebrate rod phototransduction cascade from the engineering

point of view, identifies the way in which all of the relevant engineering parameters are controlled by enzyme concentrations, and gives bounds on the required numbers of enzymes. The final section summarizes the lessons of the analysis and suggests avenues for future work. The summary of the chemical kinetics equations describing the phototransduction cascade may be found in Appendix A; Appendix B discusses the Ca feedback loop of rod phototransduction; Appendix C lists relevant biochemical parameters; and Appendix D provides details of the information theoretic arguments.

BASIC ENZYMATIC AMPLIFIER

In this section we consider the basic module of an enzymatic amplifier where the input is converted into a change in the number of messenger molecules. We show that this amplifier can be characterized by a static number gain and the response time. Signal transduction cascades can be understood as a series of such modules coupled to each other.

Let us begin by considering the basic step of chemical signal transduction: the mechanism by which the input signal—a change in the concentration of some messenger molecule—modulates the activity of the effector enzyme. The detection of weak signals requires that the input signal be converted into a significant and macroscopic change in the output level. Therefore, amplification and not just faithful transduction is necessary. No stoichiometric equilibrium mechanism can, by itself, provide such amplification.

To show this, let us consider the simplest example of a generic receptor (Lauffenburger and Linderman, 1993), R , which upon binding the messenger ligand L undergoes conformational change to an enzymatically active state R_L^* . Consider how a small change in the total number of ligand molecules may be detected. In response to a small change in the total number of ligands, dL_{tot} , no more than that many additional activated receptors, dR_L^* , can be produced. Thus, the number gain, $g_0 = dR_L^*/dL_{\text{tot}}$, is necessarily smaller than 1. (Changing the stoichiometry and going to cooperative binding of n ligands (i.e., high Hill coefficient) may offer higher sensitivity to the fractional changes of the input $d \ln[R_L^*]/d \ln[L] = n$. However, in this case the gain is even lower: $dR_L^*/dL < 1/n$.)

The amplification can be achieved in an enzymatic push-pull loop (Stadman and Chock, 1977; Koshland et al., 1978) where a messenger X is activated to X^* in a nearly irreversible reaction (e.g., phosphorylation or GDP/GTP exchange) catalyzed by an activating enzyme E_a and X^* is deactivated back to X via another nearly irreversible reaction (e.g., hydrolysis) catalyzed by a deactivating enzyme E_d (see Fig. 1). The push-pull module is described by

$$\frac{d}{dt} X^* = \Gamma_a X - \Gamma_d X^*, \quad (1)$$

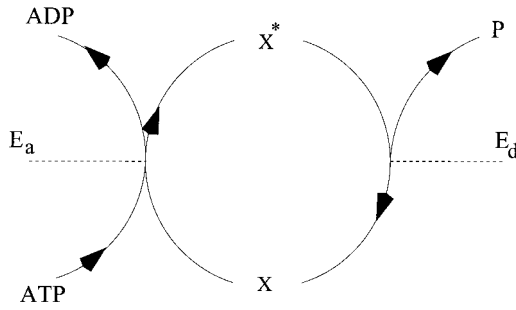


FIGURE 1 Schematic representation of a push-pull amplifier loop. The messenger molecule X is activated to the by enzyme E_a and deactivated by enzyme E_d . The activation-deactivation cycle is driven by ATP as a metabolic energy source.

where $\Gamma_{a,d}$ are the rates of activation and deactivation which depend on the concentrations of the enzymes and substrates. We shall arbitrarily take the activating enzyme E_a (which controls the activation rate Γ_a) to be the input signal. We will show that the response of X^* to small modulations in the input, E_a , are characterized by the static gain g_0 and the time constant τ . In this case, g_0 can be made as large as one wants because a single signal molecule can excite many messenger molecules. However, as we will see, this comes at the cost of increasing τ and the energy consumption.

In the simplest case of Michaelis-Menten kinetics one would have

$$\Gamma_a = \frac{k_a[E_a]}{1 + K_a^{-1}[X]}, \quad (2)$$

with K_a being the Michaelis constant and k_aK_a being the catalytic velocity. The dependence of the reaction on the concentration of energy-supplying molecules (e.g., ATP/ADP or GTP/GDP) is subsumed into the effective reaction rate k_a . We assume the reaction to be far from equilibrium and proceed unidirectionally. Here and in Eq. 1 $[A]$ denotes the concentration of molecule A , while A refers to the total number: $A = [A] * \text{Volume}$. The deactivation rate Γ_d is taken to be of the same form as Eq. 2 but dependent on $[E_d]$ and $[X^*]$ with different parameters, k_d and K_d . Finally, Eq. 1 is supplemented by a constraint on the total number of the messenger molecules $X + X^* = X_{\text{tot}}$.

In the steady state,

$$\bar{X}^* = \frac{\Gamma_a X_{\text{tot}}}{\Gamma_a + \Gamma_d} \approx \frac{k_a[\bar{E}_a]X_{\text{tot}}}{k_a[\bar{E}_a] + k_d[\bar{E}_d]}, \quad (3)$$

where the quantities with bars represent their steady-state values. The approximate expression holds for low substrate concentrations, when the saturation effects are negligible. Below, for the sake of simplicity, we shall restrict ourselves to this regime (unless stated otherwise).

Note that the ratio of active and inactive messenger concentrations in the steady state depends on the ratio of

enzyme concentrations: $[\bar{X}^*]/[\bar{X}] = k_a[\bar{E}_a]/k_d[\bar{E}_d]$. This steady state must be contrasted with the thermodynamic equilibrium, where this ratio would be fixed by the free energy difference and thus would be independent of $[\bar{E}_{a,d}]$. Thus the signal transduction capability of this enzymatic circuit is entirely due to its nonequilibrium, dissipative nature. Each activation-deactivation event dissipates ΔG_{cycle} worth of energy; our neglect of reverse reactions is consistent only to the extent that this energy is large compared to $k_B T$ (where k_B is the Boltzmann constant and T is temperature). The total power dissipation in the steady state is

$$P = \Delta G_{\text{cycle}} \Gamma_a \bar{X}. \quad (4)$$

Let us now consider the enzymatic circuit set in a certain steady state—i.e., at a certain “operating point”—and consider the behavior of small deviations about it: $\Delta X^* \equiv X^* - \bar{X}^*$ in response to small fluctuations of the “input,” $\Delta E_a \equiv E_a - \bar{E}_a$. Linearizing Eq. 1 yields

$$\frac{d}{dt} \Delta X^* = -\tau^{-1}(\Delta X^* - g_0 \Delta E_a), \quad (5)$$

where

$$\tau \equiv \left(\frac{\Gamma_a}{1 + K_a^{-1}[\bar{X}]} + \frac{\Gamma_d}{1 + K_d^{-1}[\bar{X}^*]} \right)^{-1} \approx (k_a[\bar{E}_a] + k_d[\bar{E}_d])^{-1} \quad (6)$$

is the time constant of the response which controls how fast the perturbation decays back to the steady state and

$$g_0 \equiv \frac{d\bar{X}^*}{d\bar{E}_a} = \frac{\tau k_a[\bar{X}]}{1 + K_a^{-1}[\bar{X}]} \approx \tau k_a[\bar{X}] \quad (7)$$

is the differential static gain, defined as the change in the steady state \bar{X}^* in response to a small increment in \bar{E}_a . Equation 5 can be solved explicitly by Fourier transform. The response to input modulation at frequency ω : $\Delta E_a(t) = \int d\omega e^{i\omega t} \Delta \hat{E}_a(\omega)$ defines frequency-dependent gain:

$$g(\omega) \equiv \frac{\Delta \hat{X}^*(\omega)}{\Delta \hat{E}_a(\omega)} = \frac{g_0}{1 + i\omega\tau}. \quad (8)$$

(Note that $g(\omega)$ is defined as a complex number, the phase of which fixes the time lag between the input and output oscillations.) The amplitude of the frequency-dependent gain decreases rapidly at frequencies higher than τ^{-1} , so that high amplification is limited to the frequencies within a bandwidth $\Delta\omega = \tau^{-1}$. The maximal gain g_0 is achieved at $\omega = 0$. Note that both g_0 and τ depend on the operating point of this enzymatic amplifier, which is characterized by $(\bar{X}, \bar{E}_a, \bar{E}_d)$. From Eq. 8, we see that small, time-dependent

variations in E_a produce changes in X^* according to

$$\Delta X^*(t) = g_0 \int_{-\infty}^t dt' e^{-(t-t')/\tau} \Delta E_a(t'). \quad (9)$$

The beauty and the presumed evolutionary advantage of the push-pull scheme are in its tunability. Assuming $k_{a,d}$ and $K_{a,d}$ to be fixed molecular “hardware” parameters leaves the concentrations $[\bar{E}_{a,d}]$, $[\bar{X}_{tot}]$ available for tuning. For example, the ratio $[\bar{E}_a]/[\bar{E}_d]$ controls the fraction of activated messenger $[\bar{X}^*]/[\bar{X}_{tot}]$ in the steady state, while the response time constant may be tuned independently by scaling both $E_{a,d}$ concentrations up or down. The gain may be increased in two ways: 1) by decreasing enzyme concentrations $[\bar{E}_{a,d}]$ and thereby increasing the time constant, or 2) by increasing the total messenger concentration $[\bar{X}_{tot}]$ and hence $[\bar{X}]$. Increasing τ corresponds to the longer lifetime of the active messenger, resulting in larger cumulative changes in X^* in response to a change in E_a . However, long τ also means that the X^* cannot follow rapid changes in E_a : high gain comes at the expense of sluggish behavior. The compromise between high gain and fast response is quantified by the gain-bandwidth product, $g_0\tau^{-1}$, which is bounded because

$$g_0\tau^{-1} = \frac{k_a[\bar{X}]}{1 + K_a^{-1}[\bar{X}]} < k_a K_a. \quad (10)$$

The product $K_a k_a$ is just the catalytic velocity of the enzyme. Increasing $[\bar{X}_{tot}]$ and therefore $[\bar{X}]$ regulates the gain directly but ineffectively once the saturation regime $[\bar{X}] > K_a$ is reached. Also from (4) it is clear that scaling up the total messenger concentration increases the rate of dissipation.

Phototransduction cascade provides two examples of enzymatic amplifier loop (Stryer, 1995) (see Figs. 2 and 3). In its first (membrane) stage, the activated rhodopsin (Rh^*)—the photoreceptor protein—catalyzes GDP/GTP exchange and the consequent activation of α -transducin, G_α^* (a member of the G-protein family). The deactivation of G_α^* via GTP hydrolysis is catalyzed by the inhibitory subunit of the phosphodiesterase PDE_γ to which G_α^* binds. Thus G_α plays the role of X , Rh^* plays the role of E_a , and PDE_γ plays the role of E_d . Of course, viewed in full detail, the G-protein mechanism is more complex than the push-pull cartoon: in particular, the loop involves the release and recovery of $G_{\beta\gamma}$ subunits. This complication, however, is inessential (which does not mean that $G_{\beta\gamma}$, itself in many cases (Stryer, 1995) acting as a messenger, is irrelevant!), while the presence of the activation/deactivation loop powered by the out-of-equilibrium GTP/GDP ratio is fundamental.

The “readout” of the G-protein stage (see Fig. 3) is provided via the activation of the catalytic subunit of PDE through G_α^* - PDE_γ binding. Active PDE^* enzymatically hydrolyzes cGMP—the active messenger of the second (cytoplasmic) stage—down to GMP. cGMP is resynthesized by a guanylyl cyclase (GC) from the constant supply of GTP

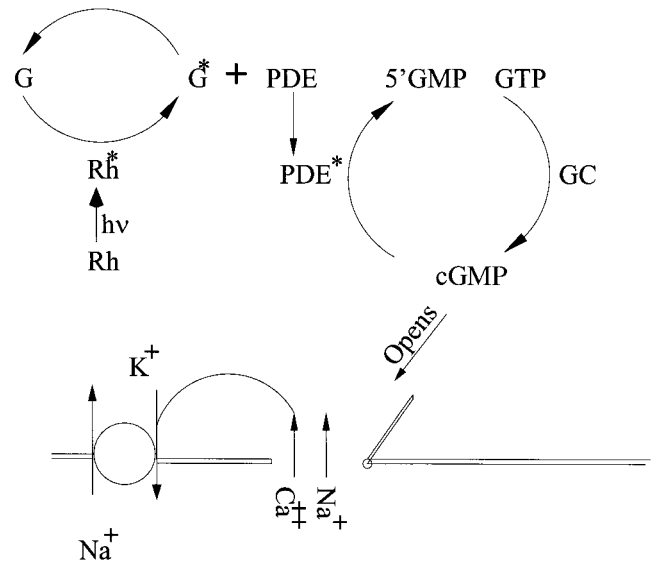


FIGURE 2 Phototransduction cascade. The incident photon activates rhodopsin, which in turn activates G-protein to form G_{GTP}^* . The activated G-protein binds to PDE and activates it, PDE^* . These reactions take place on the surface of a disc. Activated PDE hydrolyzes cGMP in the cytoplasm. The drop in cGMP concentration causes some of the cyclic nucleotide-gated channels in the surface membrane of the outer rod segment to close, reducing the current into the cell and repolarizing it. Synthesis of cGMP by GC restores its concentration.

and plays the role of X^* in Eq. 1. Even though in this case the full messenger activation/deactivation loop, $GTP \rightarrow cGMP \rightarrow GMP$, is only closed via a metabolic pathway, the quantitative analogy with the “push-pull” scheme is unmistakable. The quantitative description of the two-stage phototransduction cascade may be found in Appendix A; we shall discuss its engineering aspects in detail in the section Enzymatic Amplifier Cascade in Phototransduction.

FLUCTUATIONS AND NOISE

Chemical reactions are stochastic processes, and hence there are random fluctuations in the number of excited messenger molecules. The noise caused by these fluctuations determines how small a signal can be transduced faithfully. The design of any signal transduction system cannot be understood without considering its noise characteristics.

To that end, let us describe the fluctuations in the push-pull amplifier loop illustrated in Fig. 1. This amplifier loop consists of a forward reaction, exciting the messenger X at a rate r_+ , and a backward reaction involving the deexcitation of X^* at a rate r_- . In Eq. 1, r_+ is just $\Gamma_a X$ and r_- is $\Gamma_b X^*$. The fluctuations in the number of X and X^* molecules are due to the Poisson nature of chemical reactions. Let us say that during a time interval Δt , the forward reaction produces n_+ more molecules, while the backward reaction leads to a loss of n_- molecules of X^* . The net production of

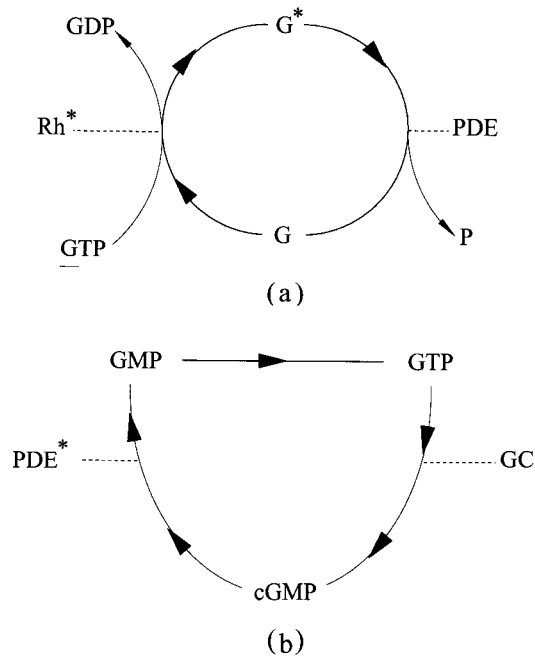


FIGURE 3 The two amplifying modules in phototransduction. (a) Activated rhodopsin catalyzes activation of transducin (the G-protein). This loop is powered by the GTP-GDP hydrolysis. (b) Active phosphodiesterase hydrolyzes cyclic GMP to 5'-GMP; cGMP is synthesized by GC; the loop is closed by the metabolic process which maintains GTP concentration.

X^* is $n_+ - n_-$. The forward and backward reactions are independent statistical processes. The average number of X^* produced is just $\langle n_+ - n_- \rangle = (r_+ - r_-)\Delta t$. Because these processes are Poissonian, the variance of n_+ is $\langle (n_+ - \langle n_+ \rangle)^2 \rangle = \langle n_+ \rangle = r_+ \Delta t$, and, similarly, that of n_- is $\langle (n_- - \langle n_- \rangle)^2 \rangle = \langle n_- \rangle = r_- \Delta t$. The variance of the total increment of X^* is the sum of the two variances, i.e., $(r_+ + r_-)\Delta t$. This statistical behavior can be captured mathematically by introducing a time-dependent random noise variable $\eta(t)$ into the chemical kinetics equation (Eq. 1),

$$\frac{d}{dt} X^* = \Gamma_a X - \Gamma_d X^* + \eta(t), \quad (11)$$

written here for the total number of molecules in a fixed volume. When this number is large and on a time scale longer than the microscopic time scale (time scales of order $1/(r_+ + r_-)$, on which single molecules are produced), $\eta(t)$ is a Gaussian random function of time with a zero average $\langle \eta(t) \rangle = 0$ and a “white noise” autocorrelation:

$$\langle \eta(t)\eta(t') \rangle = (\Gamma_a X + \Gamma_d X^*)\delta(t - t') \quad (12)$$

(where, $\delta(z)$ is a Dirac delta function whose value is zero everywhere except in the infinitesimal vicinity of $z = 0$ and whose integral over z is 1. The coefficient of the delta function, which is the strength of the noise, is determined by equating $\langle \int^{\Delta t} d\eta(t) \int^{\Delta t} dt' \eta(t') \rangle$ to $(\Gamma_a X + \Gamma_d X^*)\Delta t$, which

is the total variance of increment of X^* during the interval Δt . Equation 11 could be written more generally for the spatially dependent concentrations with the inclusion of molecular diffusion, but here we will neglect this effect. Small stochastic fluctuations about the uniform steady state (Eq. 3) δX^* are governed by the linearization of Eq. 11:

$$\frac{d}{dt} \delta X^* = -\tau^{-1}(\delta X^* - g_0 \delta E_a) + \eta(t). \quad (13)$$

This equation is very similar in structure to Eq. 5, except that δE_a stands for the noise in the input. The contribution to the variance of the fluctuations, $\delta X^*(t)$, due to $\eta(t)$ is

$$\langle (\delta X^*)^2 \rangle = \frac{1}{2} \tau (\Gamma_a \bar{X} + \Gamma_d \bar{X}^*) = \frac{\tau}{\Gamma_a^{-1} + \Gamma_d^{-1}} X_{\text{tot}}, \quad (14)$$

with $\langle \rangle$ representing the average over the noise η . This expression can be obtained using Eq. 12, and the fact that $\bar{X} = X_{\text{tot}} \Gamma_d / (\Gamma_a + \Gamma_d)$ and $\bar{X}^* = X_{\text{tot}} \Gamma_a / (\Gamma_a + \Gamma_d)$. Note that here we have not included the fluctuations in the number of the activating/deactivating enzymes. If substrate saturation can be neglected in the enzymatic rates, expression (14) for the variance reduces to $(1/X + 1/X^*)^{-1}$, which also holds in equilibrium. Since X^* serves as a “readout,” the left-hand side of Eq. 14 is identified as the output noise N_{out} . Note that the r.m.s. fluctuation normalized to the mean $\sqrt{\langle (\delta X^*)^2 \rangle} / \bar{X}^*$ decreases with increasing total messenger number, X_{tot} . Of course, just like an increase in the gain-bandwidth product, noise reduction comes at a price of increasing energy dissipation, because the number of activation/deactivation events per unit time increases with X_{tot} .

In addition to the above output noise, the total variance of X^* includes the contribution of the fluctuation in the enzyme number, δE_a , which is amplified by the gain factor and should be thought of as the input noise of the amplifier. The total variance is given by

$$\langle (\delta X^*)^2 \rangle_{\text{tot}} = \int \frac{d\omega}{2\pi} |g(\omega)|^2 \langle |\delta \hat{E}_a(\omega)|^2 \rangle + N_{\text{out}}. \quad (15)$$

Here, N_{out} is given by Eq. 14, $\langle |\delta \hat{E}_a(\omega)|^2 \rangle$ is the power spectrum of the fluctuations in number of active input enzymes, and $g(\omega)$, given by Eq. 8, is the frequency-dependent gain. For example, if the activating enzyme is itself governed by the push-pull process with a time constant τ_{E_a} , one would have $\langle |\delta \hat{E}_a(\omega)|^2 \rangle = 2\tau_{E_a} \langle \delta E_a^2 \rangle / (1 + \omega^2 \tau_{E_a}^2)$. The frequency integral in Eq. 15 reflects the low-pass filtering property of the X^* response: the magnitude of the gain $|g(\omega)|^2 = g_0^2 / (1 + \tau^2 \omega^2)$ decreases with ω . If the bandwidth of the amplifying stage, τ^{-1} , is small compared with the bandwidth of input fluctuations, $\tau_{E_a}^{-1}$, input noise variance will be suppressed by a factor of τ_{E_a} / τ . This is just the effect of time averaging, because, in that case, the amplifier response sums over τ/τ_{E_a} independent samples of the input.

Noise reduction can be achieved at the price of sluggish response, i.e., by increasing τ .

ENZYMATIC CASCADE

Why does cellular signal transduction often involve multiple steps? The primary engineering benefit of having a cascade of amplifiers is the ability to achieve higher gain without compromising the time constant of the response. Consider, for example, a cascade constructed from a sequence of enzymatic loops (Chock and Stadman, 1977) (Eq. 1), with the identification of the activated messenger output $X^{(n)*}$ of the n th stage with the “input” enzyme of the $n + 1$ st stage, $E_a^{(n+1)}$. Each stage is endowed with its own set of kinetic parameters $k_{a,d}^{(n)}$ (and $K_a^{(n)}$) and tunable $X_{\text{tot}}^{(n)}$ and $E_d^{(n)}$. With the latter two parameters per stage one can control both the time constant τ_n (via $E_d^{(n)}$) and the static gain, $g_0^{(n)} = \tau_n(k_a^{(n)}[\bar{X}^{(n)}]/(1 + (K_a^{(n)})^{-1}[\bar{X}^{(n)}]))$ in each stage. If the cascade performance specifications require a certain overall zero frequency gain, \tilde{g}_0 , how should the parameters of the individual stages be set to achieve maximum bandwidth for the cascade?

As long as we consider only linear response to small inputs, the overall gain of the cascade is just the product over the stages:

$$\tilde{g}(\omega) = \prod_{n=1}^{n_c} g^{(n)}(\omega) = \prod_{n=1}^{n_c} \frac{g_0^{(n)}}{1 + i\tau_n\omega}, \quad (16)$$

where n_c is the number of cascade stages. Our requirement for the overall gain implies $\prod_{n=1}^{n_c} g_0^{(n)} = \tilde{g}_0$. Because each of the stages obeys the bound (Eq. 10), we obtain a constraint on the time constants,

$$\prod_{n=1}^{n_c} \tau_n^{-1} \leq \frac{\prod_{n=1}^{n_c} k_a^{(n)} K_a^{(n)}}{\tilde{g}_0}. \quad (17)$$

We can generally define the overall time constant as the maximum of the time constants of the individual stages, i.e.,

$$\tilde{\tau} = \max(\tau_1, \dots, \tau_n). \quad (18)$$

The total bandwidth, $\tilde{\tau}^{-1}$, is maximized, under the constraint of Eq. 17, by making all time constants equal:

$$\tau_n = \tilde{\tau}.$$

Thus, the maximum bandwidth, which is achieved by setting all of the time constants to be equal, is

$$\tilde{\tau}^{-1} = \frac{(\prod_{n=1}^{n_c} k_a^{(n)} K_a^{(n)})^{1/n_c}}{\tilde{g}_0^{1/n_c}}.$$

When the catalytic velocities, $k_a^{(n)}K_a^{(n)}$, are all comparable, increasing the number of stages, n_c , increases the bandwidth or equivalently decreases the response time. The “speed”

comes at a price of higher energy dissipation in the case of the cascaded amplifier because every stage requires an energy supply.

Another hidden “cost” of the cascade is the noise. As we have seen in the previous section, the gain in each stage has to be sufficiently large for the signal-to-noise not to deteriorate because of the shot noise introduced in every stage. That precludes the temptation to build a cascade with a large number of steps and a small gain per stage.

ENZYMATIC AMPLIFIER WITH FEEDBACK

Response characteristics of the amplifier may be controlled and modified via feedback. Imagine, for example, that the output $[X^*]$ of the push-pull circuit affects the “production” or influx of molecular species C :

$$\frac{d}{dt}[C] = -\tau_C^{-1}[C] + F([X^*]), \quad (19)$$

which in turn regulates the activity of, say, deactivating enzyme, so that $E_d = E_d^{\text{tot}}H([C])$ (i.e., only a fraction, $H([C])$, of the total number E_d^{tot} are active). Function F in (19) denotes the influx (or production) of C , and τ_C^{-1} denotes the rate of its outflux (or destruction). In phototransduction, as well as in many other cases, the feedback signal is Ca^{2+} (see Appendix A), which regulates enzymatic activity via an intermediary Ca-binding proteins. Including the C dependence in Eq. 1 and linearizing it together with (19) yields

$$\tau \frac{d}{dt} \Delta X^* = -\Delta X^* + g_{\text{xc}} \Delta C + g_0 \Delta E_a \quad (20)$$

$$\tau_C \frac{d}{dt} \Delta C = -\Delta C + g_C \Delta X^* \quad (21)$$

with $g_{\text{xc}} = -\tau k_d [E_d^{\text{tot}}] \bar{X}^* dH/d[C]$ and $g_C = \tau_C dF/d[X^*]$. The above equations can be solved using Fourier transforms. The response of ΔX as a function of ΔE_a in Fourier space is given by

$$\Delta \hat{X}(\omega) = g_f(\omega) \Delta \hat{E}_a(\omega),$$

with the effective gain, g_f , given by

$$g_f(\omega) = \frac{g_0(1 + i\omega\tau_c)}{-\tau\tau_c\omega^2 + i\omega(\tau + \tau_c) + 1 - g_C g_{\text{xc}}}. \quad (22)$$

At very low frequencies the gain is

$$g_f(0) = \frac{g_0}{Y}. \quad (23)$$

Therefore the static gain is divided by a gain reduction factor,

$$Y = 1 - g_C g_{\text{xc}}. \quad (24)$$

Negative feedback corresponds to either g_{xc} or g_c negative, so that $g_{xc}g_c < 0$ and $Y > 1$, in which case the effective static gain is reduced.

Because of the additional dynamical variable, C , the temporal response of ΔX^* becomes more complex and involves two time constants. Consider the response to a small step in ΔE_a . Suppose for simplicity $\tau_c \gg \tau$. In that case the feedback effect is slow and the response peaks at $\Delta X_{\text{peak}}^* \approx g_0 \Delta E_a$ (the static response value without feedback) at the time of order τ . Relaxation to the lower, asymptotic value, $\Delta X_s^* = g_f(0) \Delta E_a$, occurs as the feedback switches on, on the time scale of $\tau_{\text{fbk}} = \tau_c / Y$. In the opposite limit of fast feedback, $\tau_c \ll \tau$, there is no peak in the step response, which goes directly toward ΔX_s^* with a time constant τ / Y . The two limits are compared in Fig. 4. (For $\tau \approx \tau_c$ the system has damped oscillatory response.)

The static input-output map $X^*(E_a)$ and the dependence of the differential gain on the signal level involve the details of feedback coupling, $F([X^*])$ and $E_d^{\text{tot}}H([C])$.

We saw here that the feedback loop is characterized by two parameters: the feedback factor Y and the time constant τ_c . In the case of Ca feedback (discussed in Appendix A) the latter is controlled by the number of Na/K/Ca exchangers which pump Ca out of the cell. The gain, on the other hand, is controlled by the number of Ca-binding proteins which mediate its effect on the push-pull loop enzyme (guanylyl cyclase in the case of phototransduction). Most significantly, the introduction of feedback allows one to decouple the fast and slow responses by introducing a slow time scale. In the case of phototransduction, the slow time scale is associated not with Ca recovery τ_c (as in the above example) but with the intermediate Ca-binding proteins acting as Ca buffers (see Appendix B).

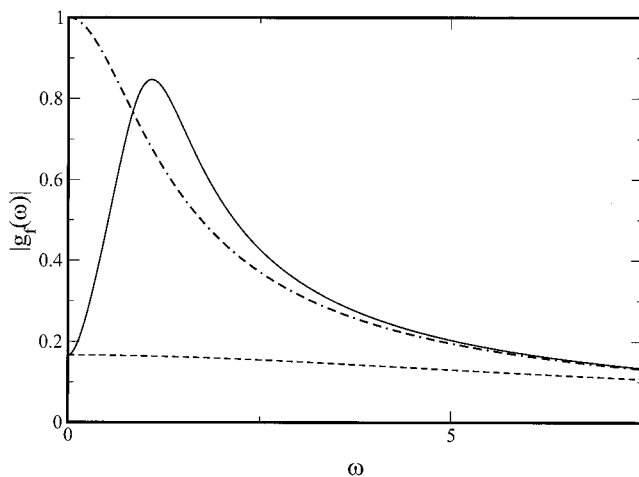


FIGURE 4 Frequency response with feedback: amplitude of the frequency-dependent gain, $|g_f(\omega)|$, as a function of frequency, ω . Slow feedback response, i.e., large τ_c , is shown by the solid line; the fast feedback response is shown by the dashed line; and the case with no feedback is shown by the dot-dashed line.

MINIMAL REQUIRED GAIN AND MINIMAL MESSENGER CONCENTRATION

How much gain should a signal transduction cascade have? The input signal must generate a significant change at the output, which means a change that is unlikely to be produced by a spontaneous fluctuation of the output substance. Hence, amplification must be sufficiently strong for the signal to be larger than the root mean square (r.m.s.) noise of the output, $\sqrt{N_{\text{out}}}$. On the other hand, the minimal significant input signal is set by the r.m.s. input noise $\sqrt{N_{\text{in}}}$. (Here, N_{in} is not quite the fluctuations in the input but includes the frequency dependence of amplification and is defined as $\int (d\omega/2\pi) \langle |\delta \hat{E}(\omega)|^2 \rangle / (1 + \omega^2 \tau^2)$.) Detectability of this signal requires

$$g_0 > \frac{\sqrt{N_{\text{out}}}}{\sqrt{N_{\text{in}}}}, \quad (25)$$

which puts a lower bound on required gain. Of course, the noise may always be reduced by increasing the time constant τ of the amplifier, but this comes at a price of a sluggish response to interesting stimuli. Therefore in our discussion we assume τ to be fixed at its upper bound determined by the temporal response requirements. Under this condition, both signal and noise in X^* fluctuate with the same time scale, namely τ . Thus, further filtering of this output does not improve signal detection.

For the push-pull enzymatic circuit, the input noise would be set by spontaneous fluctuations of the input enzyme concentration $\langle \delta[E_a]^2 \rangle$ and the output noise by $\langle \delta[X_*]^2 \rangle$. Because gain is proportional to the concentration of messenger molecules, Eq. 25 implies a lower bound on the required messenger concentration:

$$[X] > \frac{1}{\tau k_a} \sqrt{\frac{N_{\text{out}}}{N_{\text{in}}}} \quad (26)$$

(with the saturation effect included, one finds that Eq. 26 can be satisfied only if $\sqrt{N_{\text{out}}/N_{\text{in}}}$ does not exceed the maximal gain $\tau k_a K_a$ (Eq. 10). Note that although the variance of both input and output noise scales linearly with the total number of participating molecules (as appropriate for a Poisson process), their ratio depends only on concentrations and is independent of the cell volume. Let us estimate N_{out} according to Eq. 14 and assume for simplicity that the time constant of δE_a fluctuations, τ_{E_a} , is equal to τ , so that $N_{\text{in}} \approx \langle \delta E_a^2 \rangle$. In the regime below saturation, $[\bar{X}] \approx \tau k_d [\bar{E}_d] [X_{\text{tot}}]$ (according to Eq. 3), and one finds explicitly

$$[X_{\text{tot}}] > \frac{1}{\tau k_a} \frac{1}{\tau k_d [\bar{E}_d]} \frac{\bar{E}_a}{\langle \delta E_a^2 \rangle}. \quad (27)$$

Note that the right-hand side of Eq. 27 depends on the "operating point," i.e., the steady-state concentrations $[\bar{E}_a]$. In the limit of $[\bar{E}_a] \rightarrow 0$, $\tau^{-1} \approx k_d [\bar{E}_d]$ from Eq. 6 and with

the Poisson statistics assumption ($\langle \delta E_a^2 \rangle = \bar{E}_a$), the bound reduces to $[X_{\text{tot}}] > k_d \bar{E}_d / k_a$. We shall return to this inequality and the role it plays in constraining the relative abundance of enzymes in a signal transduction cascade in the section Enzymatic Amplifier Cascade in Phototransduction.

OPTIMIZATION OF INPUT/OUTPUT RELATION AND ADAPTATION

In the previous section we established the lower bound on the gain necessary to resolve the smallest significant input. More generally, one must consider the performance of the transduction system over the full range of stimuli. It is typically desirable to transduce as broad a dynamic range of the input signal as possible. Setting the amplification gain too high is bad, as it will reduce the dynamic range by causing the output to saturate. While detectability of weak stimuli puts a lower bound on the differential gain at low background stimulus, the dynamic range consideration constrains the gain over the whole input range. Under conditions of a wide input dynamic range, a compromise between the two is required. The optimal input/output relation for a transduction system is determined by information theoretic considerations (Cover and Thomas, 1989), which formalize and extend the argument given in the previous section. Some of the details are relegated to Appendix D.

Generalizing the discussion in the previous section, we consider signal transduction as a mapping of an input variable, say y , measurable with an accuracy set by the r.m.s. noise $\sqrt{N_{\text{in}}(y)}$ to an output variable $z = f(y)$ measurable with accuracy $\sqrt{N_{\text{out}}(z)}$. In phototransduction, the input is the light intensity with the measurement uncertainty set by the photon shot noise, and the output is the neurotransmitter with uncertainty set by shot noise in the vesicle release. Information theoretically, the “quality” of signal transduction can be quantified via mutual information, which measures the degree of certainty about the input value y gained from observing output z . The optimal input/output mapping is the one which maximizes this mutual information. It depends not only on the noise properties but on the statistical distribution of inputs, i.e., probability $P(y)$ of input value being between y and $y + \delta y$. The r.m.s. noise levels, $N_{\text{in}}^{1/2}(y)$ and $N_{\text{out}}^{1/2}(z)$, define just noticeable differences in y and z , respectively, and provide the natural units for these quantities; e.g., $dy/N_{\text{in}}^{1/2}(y)$ counts the number of distinguishable input states in a small interval dy . In the limit where the number of distinguishable output states is much smaller than the number of distinguishable input states, it has been demonstrated (Laughlin, 1981) that the optimal input/output mapping is the one which makes all distinguishable states of the output occur with equal probability. The latter is achieved if $z(y)$ is chosen to satisfy $dz/dy = cN_{\text{out}}^{1/2}(z)P(y)$ (with the constant c fixed by imposing the output dynamic range constraint: $\int dy dz/dy = z_{\text{Max}}$).

To illustrate the relation of the input signal statistics with the optimal input/output relation, let us consider the case of phototransduction under the high light (photopic) conditions handled by the cones. It has been argued forcefully (e.g., see Shapley, 1989) that the natural variation in light intensity is due to the variable reflectivity of objects and hence occurs on a logarithmic scale. Assuming for the number of photons absorbed per characteristic time τ a log-normal distribution $P(y) = (\sqrt{\pi\sigma y})^{-1} \exp(-\sigma^{-2}(\ln(y/\bar{y}))^2)$ (parameterized by the median intensity \bar{y} and a dimensionless variance $\sigma \approx 1$) would lead to an input/output relation with the form $z \approx z_0 \ln(y/\bar{y}) + \text{const.}$, in some intermediate range of y . This implies $dz/dy \approx z_0/y$, i.e., progressive desensitization with increasing input intensity. The latter is known empirically as the Weber law (Naka et al., 1987; Normann and Perlman, 1979).

Now suppose that the statistical properties of the input vary slowly in time. For example, the statistics of light intensity may be measured over a single scene but will change slowly as the sun rises. Instead of “tuning” the response on the basis of the full-time independent distribution, which lumps together the intensity data at all times of day, it would be beneficial to tune in accordance with the “current conditions” quantified by the short-term statistics. The slow time evolution of the short-term statistics is plausibly well parameterized by mean intensity (over immediate past), which is readily measurable. To remain optimal at all times, the input/output mapping of the transduction cascade must be able to change along with the change in the input distribution—the system must adapt—and equation relating the desired input/output relation with input statistics gives a precise and quantitative definition of optimal adaptation. The notion of adaptation as a slow change in the input/output mapping in response to a change in input statistics must be contrasted with the dependence of the differential response on input level, which simply reflects the nonlinearity of the input/output mapping. Adaptation in general must also not be confused with the often desirable property of not responding to static input; e.g., gradient detection in bacterial chemotaxis requires a purely transient response, which is often referred to as “absolute adaptation” (Koshland et al., 1978).

To confront this engineering view of adaptation with biological reality, we replot in Fig. 5 the data of Normann and Perlman (1979) for the turtle cone voltage response to light pulses on different light backgrounds, I_b , and compare it with the input/output curves optimized for the log-normal distribution, $P(I/\bar{I})$, parameterized by its median \bar{I} . Ignoring variation in the base level and saturation voltages, the response curves are related by a horizontal shift parameterized entirely by \bar{I} . This shift of the response is the adaptation effect and may be accounted for by a change in overall cascade gain. However, while for the intermediate background intensities the response is close to optimal, the readjustment of the median response $V(\bar{I})$ is smaller than

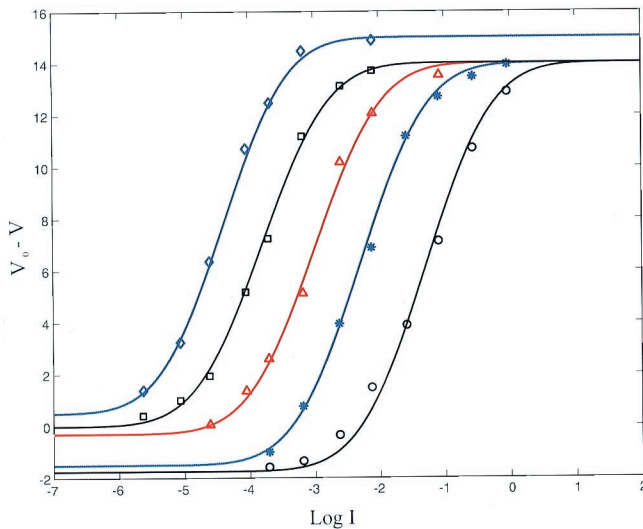


FIGURE 5 Adaptation in turtle cones: adaptation data for turtle cones from Normann and Perlman (1979). Points correspond to a peak voltage response to short pulses with intensity I (in arbitrary units) superimposed on the steady backgrounds. \diamond , Dark-adapted response; \square , $\ln I_b = -4.4$; \triangle , $\ln I_b = -3.2$; $*$, $\ln I_b = -2.1$; \circ , $\ln I_b = -1$. Fitting curves have the form of the optimal input/output function for log-normal input intensity distributions: $V(I) = a \text{Erf}(\sigma^{-1} \ln(I/\bar{I})) + b$. Parameter $\sigma = 1.15$ is the same for all fits, while a and b adjust for the drift of the base and the saturation voltage of the experiment. The horizontal translation of the fitting functions is controlled by \bar{I} . Data in order of increasing I_b fit by curves with $\ln \bar{I}$ are -4.4 , -3.8 , -3 , -2.3 , -1.3 . To the extent that \bar{I} is not exactly the background intensity, adaptation is not perfect.

what would be expected for the ideal adaptation to the input with median intensity I_b . The adaptation is imperfect!

ENZYMATIC AMPLIFIER CASCADE IN PHOTOTRANSDUCTION

We have already invoked phototransduction as an example at several key points of our discussion. In brief, phototransduction (Stryer, 1995) in retinal rods and cones of the vertebrates involves down-regulation of neurotransmitter release in response to light which proceeds via a number of steps, as shown in simplified form in Fig. 2. Photoactivated rhodopsin, Rh^* , catalyzes GDP/GTP exchange activating transducin- α , G^* , which in turn activates phosphodiesterase (PDE)—this, as discussed earlier, constitutes the first stage of amplification. In the second stage, the increased activity of PDE reduces the concentration of cyclic GMP, causing the closure of cGMP-gated Na channels and the repolarization of the cell. The response recovery involves deactivation of the Rh^* , which proceeds via phosphorylation by rhodopsin kinase followed by arrestin binding. The complex of transducin- α with the inhibitory subunit of PDE decays via hydrolysis of bound GTP, causing deactivation of PDE. The concentration of cGMP is restored through the action of GC. The deactivation processes are regulated by Ca concentra-

tion (Koutalos and Yau, 1996), which provides the major feedback signal; the temporary closure of the CNG channels causes a rapid drop in Ca level thanks to continuous action of the Ca/K/Na exchanger. All of the above processes, at least in rods, have been characterized in considerable quantitative detail (for reviews see Stryer, 1991; Baylor, 1996; Lamb and Pugh, 1992; Bownds and Arshavsky, 1995; Koutalos and Yau, 1996).

What determines the design characteristics of the rod cell? What are the engineering considerations which set the operating point of the amplifier, its gain, and time constant? How can the appropriate tuning be achieved through adjusting concentrations of enzymes?

Under the low light conditions relevant to rod phototransduction, the main consideration is the gain required for single photon resolution. As emphasized earlier, the minimum gain depends on the noise characteristics of different stages and ultimately on the noise in the readout, the vesicle release rate. Unfortunately, whereas the enzymatic cascade leading to repolarization of the rod outer segment (ROS) is well documented, the mechanism by which the changes in the membrane potential are transduced into the modulation of the neurotransmitter-containing vesicle release is less clear (Rieke and Schwartz, 1996). However, we will only need an order-of-magnitude estimate of the minimal significant modulation of the ROS membrane potential, and we shall circumvent the lack of detailed knowledge of the processes in the inner rod segment by assuming that relative change in the release rate is of the same order as the fractional change of ROS current (proportional to the number of open channels Ch^*).

Let us first consider the setting of the operating point of the ROS, defined by the number of channels open in the dark state and the corresponding membrane potential. Assuming each open channel has a conductance σ_{Ch} , the total conductance of the outer segment $\sigma_{\text{out}} = \sigma_{\text{Ch}} \text{Ch}^*$. The cell potential is determined by the condition that charge influx into the ROS is balanced by the charge outflux from the inner segment. Quite generally (a special case is discussed in Appendix A), $V = \nu f(R_{\text{in}} \sigma_{\text{out}})$, with membrane potential, V , defined relative to the saturation voltage corresponding to a high incident light level. V is a function of the ratio of resistance of the inner segment, R_{in} , to that of the outer segment, σ_{out}^{-1} , with ν setting the dynamic range for the variation of V . By our definition, as channel close $\sigma_{\text{out}} \rightarrow 0$ the function $f \rightarrow 0$ and $V \rightarrow \nu$ (i.e., $f \rightarrow 1$) as $\sigma_{\text{out}} \rightarrow \infty$. One expects that the half-maximum of V occurs for $R_{\text{in}} \sigma_{\text{out}} \sim o(1)$ (meaning “of order 1”). Hence, the operating point of the rod in the dark should be set so that the resistance of the outer segment is of the same order of magnitude as the resistance of the inner segment, which provides an order-of-magnitude estimate for the number of open channels in the dark: $\text{Ch}_{\text{dark}}^* \sim 1/R_{\text{in}} \sigma_{\text{Ch}}$. Based on $\sigma_{\text{Ch}} \approx 0.1$ pS (Bodoia and Detwiler, 1985) and $R_{\text{in}} \approx 0.4$ G Ω (Rieke and Schwartz, 1994), one arrives at $\text{Ch}_{\text{dark}}^* \sim 4 \times 10^3$ —quite

comparable with estimates based on resting dark current (Rispoli et al., 1993). The setting of the operating point is dictated by impedance matching! (An additional constraint is the time constant of the voltage response limited by $R_{in}C$ (where C is the membrane capacitance), which should not exceed ~ 1 s required of the overall response. Hence R_{in} cannot be too large, and therefore Ch_* and the dark current cannot be made too small.)

Next we address the issue of the minimal required cascade gain, for which we need an estimate of the readout noise. In the dark, the vesicle release rate (Rieke and Schwartz, 1996), r_v , is $\sim 10^3$ s $^{-1}$. As the intensity of light increases and the cell repolarizes, this rate eventually falls to zero. Assuming Poisson noise in the release process and a ~ 1 s time scale for the response, we estimate the minimal significant modulation to be on the order of $1/\sqrt{10^3}$, or $\sim 1/30$ of the dark rate. Because we assume that relative change in the release rate is of the same order as the fractional change in Ch^* , the minimum significant modulation of Ch^* is given by

$$\frac{\delta Ch^*}{Ch^*} \sim \frac{1}{30}. \quad (28)$$

This condition will determine the minimal required cascade gain. The fractional modulation of the open channel number compares well with experimental observations in many species (Stryer, 1991).

Let us compute the voltage response to a small change in the number of active rhodopsins. If the relevant output is the fractional change in Ch^* , we should define ‘‘photosensitivity’’ as the change in $\ln Ch^*$ in response to an incremental change in the number of active Rh receptors:

$$\frac{d \ln Ch^*}{dRh^*} = \frac{d \ln Ch^*}{dPDE^*} \frac{dPDE^*}{dRh^*}, \quad (29)$$

reflecting the multiplicative nature of gain in the cascade (see Enzymatic Cascade, above). The first and second factors on the right-hand side of Eq. 29 are directly related to the static gain factors of the cGMP and the G-protein amplification stages.

The gain factors for the two stages are calculated in Appendix A. We have

$$\frac{dCh^*}{dPDE^*} = \frac{dCh^*}{dcGMP} g_2 = 3 \frac{Ch^*}{cGMP} g_2, \quad (30)$$

where, from Eq. 41, $g_2 = \tau_{cG} k_{cG}^* [cGMP]$ is the gain of the cGMP stage (τ_{cG} is the time constant for cGMP and k_{cG}^* is the rate constant for cGMP hydrolysis by PDE*). This expression for the gain of the first stage is given by

$$\frac{dPDE^*}{dRh^*} = g_1 = \frac{\tau_H k_{Rh^*} [G]}{1 + K_G^{-1} [G]}, \quad (31)$$

where g_1 , defined in Eq. 37, is the static gain of the G-protein stage, where τ_H is the time constant for active G_α^* and k_{Rh^*} is the rate constant for G_α activation by Rh^* . Curiously, the total gain is independent of $[cGMP]$ and of the total number of channels Ch and depends only on the cell volume, Vol . This is because only the combination $Ch^{*-1} dCh^*/dPDE^* = 3\tau_{cG} k_{cG}^*/Vol$ enters (Eq. 29). The same change in the number of cGMP molecules would have a greater effect on the $[cGMP]$ and hence on the fraction of open channels if it were distributed over a smaller cell volume. In deriving the above expressions for the gain we assumed that the time constant of Ca feedback is considerably longer than the ~ 1 s characteristic time of the weak flash response. In that case the peak response can be estimated from the static gain in the absence of feedback (see Enzymatic Amplifier with Feedback, above).

Equation 28 implies a lower bound on the required amplification gain, which we shall write in the form

$$\frac{d \ln Ch^*}{dRh^*} = \frac{3\tau_{cG} k_{cG}^*}{Vol} g_1 > \frac{1}{30}. \quad (32)$$

With $\tau_{cG} \approx 1$ s and $k_{cG}^* \approx 50 \mu M^{-1} s^{-1}$, the lower bound on the gain of the G-protein stage is $g_1 > Vol(\mu m^3)/10 \approx 10^2$. The gain of the G-protein stage is given by (see Appendix A) $g_1 = \tau_H k_{Rh^*} K_{Rh^*}/(1 + K_{Rh^*} [G]^{-1})$. The maximum gain $g_{1 \text{ Max}} = \tau_H k_{Rh^*} K_{Rh^*} \approx 1000$ (where $K_{Rh} \approx 20 \mu M$ (Stryer, 1991), assuming $\tau_H \approx 1$ s) is achieved in the limit of $[G]/K_{Rh} \rightarrow \infty$. We arrive at $g_1 > 10^2$, which requires that concentration of transducin must satisfy $[G] \geq 0.1 \times K_{Rh} \approx 2 \mu M$. The reported value of $[G] \approx 100 \mu M$ (Lamb and Pugh, 1992) is well above the bound. Our bound becomes tighter if we include in the estimate the reduction of the gain due to negative feedback. The known Ca feedback pathway operating via GC reduces the gain of the second stage by factor $Y \approx 5-10$. In that case one finds $g_1 > 10^2 Y$, which implies $[G] > K_{Rh}$.

One must also compare the amplified signal to the spontaneous fluctuations. For instance, the number of G^* molecules produced by the single Rh isomerization must exceed the root mean square spontaneous fluctuation of G^* . Proceeding along the lines described above (see Minimal Required Gain and Minimal Messenger Concentration), we find that $g_1 > \sqrt{G^*}$. The rate of spontaneous (i.e., in the dark) activation of G_α is believed to be $\sim 2 \times 10^{-5}$ /s (Fawzi and Northrup, 1990). Conservatively assuming $G^*/G \approx 10^{-4}$ and taking $G = 4 \times 10^8$ (Lamb and Pugh, 1992) results in $g_1 > 200$, which as we just saw above is indeed satisfied. It is clear, however, that sufficiently low spontaneous activation of G_α is essential for single-photon detection.

Next we compare $\delta \ln V$ to the spontaneous fluctuations which arise in the outer segment. It may be shown that the thermal fluctuations of V and the fluctuations of Ch_* are irrelevant (e.g., the r.m.s. voltage fluctuations are of order $\sqrt{2k_B T/C} \approx 13 - 25 \mu V$, which is small compared to ~ 400

μV in single-photon responses. (The ROS capacitance depends on the total area of the cell membrane with a capacitance of $\sim 0.01 \text{ pF}/\mu\text{m}^2$. The total capacitance is species dependent and is $\sim 15\text{--}50 \text{ pF}$. In lizards, this is $\sim 40\text{--}50 \text{ pF}$ (Rispoli et al., 1993).) The V output noise due to the fluctuations of cGMP (Rieke and Baylor, 1996) is $(d \ln \text{Ch}^*/dc\text{GMP})\delta c\text{GMP}_{\text{r.m.s.}} \approx 3/\sqrt{c\text{GMP}} \approx 10^{-3}$ (obtained by using the observed concentration of [cGMP] in rods $\approx 5 \mu\text{M}$ or $3 \times 10^6/\text{ROS}$) (Stryer, 1991; Lamb and Pugh, 1992). Evidently this output noise is well below the required significant modulation. Had the number of cGMP molecules been less than $\sim 10^4$, this contribution to output noise would have been nonnegligible. The observed concentration of cGMP clearly satisfies the bound imposed by the minimal signal-to-noise condition. The major constraint on [cGMP] comes from the impedance matching condition discussed earlier, which fixes $\text{Ch}_{\text{dark}}^*$. Because $\text{Ch}_{\text{dark}}^* \approx \text{Ch}([\text{cGMP}]/K_{\text{cG}})^3$ (see Appendix A), reducing [cGMP] while keeping $\text{Ch}_{\text{dark}}^*$ constant would require a drastic increase in the total number of channels.

Now, let us examine the tuning of the time constants τ_{H} , τ_{cG} of the two amplification stages and of the time constant, τ_{Rh^*} , governing Rh^* shut-off. The time constants of the two amplification stages enter the gain product $g_1 g_2 \approx \tau_{\text{H}} \tau_{\text{cG}}$. In the low light regime, the gain is to be maximized. Hence, the optimal choice is to set $\tau_{\text{cG}} = \tau_{\text{H}}$ and make it as large as is consistent with the required response bandwidth τ^{-1} , as we showed earlier (Enzymatic Cascade, above). Having input $\tau_{\text{Rh}^*} > \tau$ would compromise the bandwidth, while $\tau_{\text{Rh}^*} < \tau$ would reduce the peak response to flash stimulus. (By considering the full-time dependent response one can show that the peak is controlled by the second slowest time constant. The first slowest time constant sets the recovery time scale.) We conclude that optimal tuning would be $\tau_{\text{cG}} = \tau_{\text{H}} = \tau_{\text{Rh}^*}$. The appearance of three comparable time constants corresponds to a particularly simple response time course: $(t/\tau)^2 e^{-t/\tau}$, which provides a reasonable fit to the measurements (see Fig. 6) (Baylor et al., 1974; Lamb and Pugh, 1992; Rieke and Baylor, 1998). In fact a more careful fit of the single response data from Rieke and Baylor (1998) indicates that there are four matching time constants. The possible origin of the fourth equal time constant will be discussed in an upcoming paper (Ramanathan et al., manuscript to be published). The equality of time constants provides a perspective on the debate (Nikonov et al., 1998; Pepperberg et al., 1992) concerning the limiting step in the response recovery. The disagreement in the literature stems from the observation that slowing down either the Rh^* inactivation process (increase in τ_{Rh^*}) or the hydrolysis of G_{α}^{GTP} (i.e., deactivation of G^* and increase in τ_{H}) prolongs the flash response. Both observations of course are consistent with the case of time constant matching. We emphasize that the above analysis has identified the relevant slow time scales specifically as those necessary for the achievement of sufficient gain: the detailed kinetics of the G-protein loop or

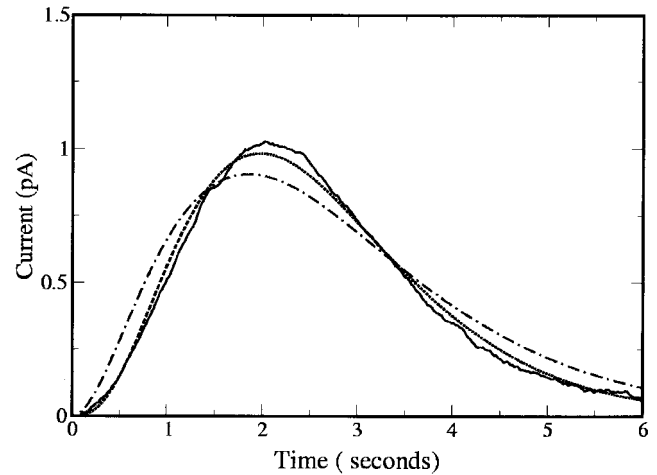


FIGURE 6 Single-photon response: measured average single-photon response of a rod cell and the fitting function. The solid curve is the experimental data from Rieke and Baylor. The dot and dashed line shows the best fit to the form $(t/\tau)^2 e^{-t/\tau}$ with $\tau = 0.92 \text{ s}$. A fit to the form, $(t/\tau)^3 \exp(-t/\tau)$, is shown by the dotted line with $\tau = 0.66 \text{ s}$.

the CNG channel would introduce many additional fast time scales which are not essential. In contrast, reducing any of the time constants τ_{cG} , τ_{H} , τ_{Rh^*} reduces the transduction gain.

Let us now consider the role of feedback. We have discussed the flash response under the simplifying assumption that the feedback time scale is much longer than the characteristic response time, $\tau \approx 1$. To be precise, in the context of the previous discussion (Enzymatic Amplifier with Feedback, above), one needs the characteristic time of the feedback to satisfy $\tau_{\text{c}} \gg 4Y\tau$. In that limit, the effect of Ca feedback only enters in the steady-state response, establishing the steady-state [cGMP]_{ss} as a function of background light intensity. The response to a step stimulus will exhibit a peak followed by slow relaxation to a new steady state—a behavior which may be thought of as adaptation. If τ_{c} is close to $4Y\tau$, there is no clear separation of time scales between the transient forward cascade and the onset of feedback. In this case, the feedback also attenuates the peak response. Thus, in general, feedback affects the response to weak flashes in two ways: 1) changes of the steady state (i.e., adaptation) and 2) direct reduction of peak response (i.e., attenuation). We have seen above that the maximum gain available in the cascade is about an order of magnitude higher than that required for single-photon detectability, which allows for a gain reduction factor $Y < 10$. It can be shown from the steady-state conditions that the introduction of feedback not only reduces the differential gain at low light intensity, but also generates a compressive nonlinearity $V \approx I^\alpha$ of the input/output relation (e.g., see Fig. 7). For example, assuming Ca feedback acting only through the GC rate, $k_{\text{GC}}(\text{Ca}) \approx [\text{Ca}]^{-n}$, yields $\alpha = 1/(n + 1/3)$, with n between 2 and 4 (Koch and Stryer, 1996). The compressive

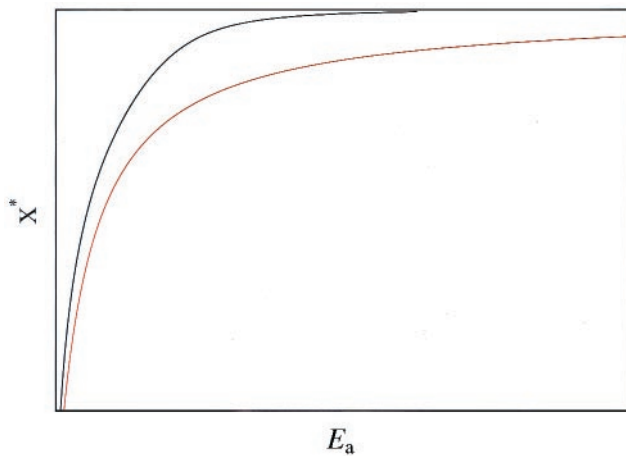


FIGURE 7 Static response with feedback: the dependence of the static input/output relationship on the feedback. The curve on the top is in the absence of feedback and saturates at a much smaller value of E_a .

nonlinearity may be desirable, as it extends the dynamic range of the flash response. This could be advantageous when there are intermittent high-intensity bursts of light on an otherwise low-light-intensity background.

Remarkably, all of the engineering parameters, gains and time constants, that have appeared in this discussion depend explicitly on the concentration of one or another molecular species and therefore can be independently tuned. We conclude this section by summarizing these dependences derived in Appendix A, in Table 1.

CONCLUSION

In the preceding sections we have attempted to present a general view of enzymatic signal transduction, first by breaking up the complex biochemistry into amplifier modules; second, by characterizing the modules in terms of the relevant engineering parameters; and third, by identifying the information theoretic considerations which govern the “tuning” of these parameters. An enzymatic push-pull circuit provides the simplest example of a chemical amplifier

and illustrates the fundamental requirement for energy dissipation and the equally fundamental tradeoff between high gain and fast response. The key engineering criterion governing the design of the amplifier concerns its noise characteristics compared with the noise level of the input signal. The enzymatic amplifier noise is due to the Poisson nature of chemical reactions and can be controlled by increasing either the total number of messenger molecules at a cost of increased dissipation or by increasing the time constant at the expense of fast response. The noise considerations lead to the minimal gain requirement and establish a lower bound on the necessary messenger concentration. These requirements are quite general in nature and arise in the information theoretic analysis of signal transduction when one attempts to determine the form of the input/output relation which maximizes the rate of information transfer.

Applying our reasoning to rod cells, we demonstrated how the engineering constraints of phototransduction at low incident light intensity can be met by a suitable choice of enzyme concentrations. It appears that all of the relevant parameters (i.e., gains and time constants) can be regulated in this way. Conversely, functional requirements put bounds on the concentrations of various enzymes. These bounds establish a domain of concentrations which provide viable engineering performance, i.e., information transfer from input to output. One could minimize energy dissipation for a given rate of information transfer by optimizing the ratio of enzyme concentrations. However, we found that such minima tend to be shallow and are likely to be superseded by other constraints arising in the process of cell development. This extended domain of viable performance may allow for diversity in the enzymatic composition of cells.

To the extent that noise-induced fluctuations are small compared with the steady-state concentrations, they can be discussed within the linear response framework (see Basic Enzymatic Amplifier, and Fluctuations and Noise, above). The minimal gain requirement is the constraint on the differential gain, i.e., amplification of small changes in the input. The consideration of weak input detectability is complemented by the considerations of the dynamic range:

TABLE 1 Parameter dependence on molecular species

Engineering parameters	Control parameter	Dependence
g_1 (Eq. 37)	$[G]$ at fixed τ_H	$\tau_H \frac{k_{Rh^*}[G]}{1 + [G]/K_{Rh^*}}$
g_2 (Eq. 41)	$[GC]$ at fixed τ_{cG} and $[Ca]$	$\tau_{cG} k_{cG}^* [cGMP]$
τ_H	[RGS9-1 protein]	Unknown
τ_{cG} (Eq. 40)	[PDE]	$(k_{PDE}[PDE])^{-1}$
τ_{Rh^*}	[Rhodopsin kinase], [arrestin]	Unknown
σ_{out} (Eq. 42)	Number of CNG channels, at fixed $[cGMP]$	$\sigma_{Ch} Ch([cGMP]/K_{cG})^3$
τ_{fbk}	[GC activating protein]	See Appendix B
Y (Eq. 47)	$[Ca]$, controlled by number of Ca/Na/K exchangers, at fixed $[cGMP]$; $[GCAP]$ via K_D (Eq. 49)	$1 + 6 \frac{[Ca]^2}{K_D^2 + [Ca]^2}$

because output saturation limits the response to strong inputs, the overall information throughput of the signal transduction system is maximized when the differential gain is kept at the minimum set by the noise level. This balance is made quantitative (Optimization of Input/Output Relation and Adaptation, above, and Appendix D) via information theory. The resulting “theoretically optimized” differential gain varies with input in a nontrivial way which depends on the statistics of external stimuli. Quite generally, the optimal input/output relation is sublinear, so that the differential gain decreases with signal level. Tailoring the shape of the input/output relation requires more tunable parameters than the simplest push-pull circuit can provide; this is achieved by a cascade of amplifier loops with negative feedback. Furthermore, as the required input/output relation depends on input statistics, better performance is achieved if the system can adapt to the prevailing conditions as they change with time (e.g., average light level). This adaptation requires that there be a “memory” of the recent input. In the simplest form, adaptation can be implemented by a feedback loop which is capable of modifying the temporal response of the amplifier and allows one to independently control the instantaneous and steady-state responses. Hence in the section Enzymatic Amplifier with Feedback, we discussed the properties of a generic enzymatic feedback circuit, and in Appendix A, the properties of one of the Ca mediated negative feedback loops in phototransduction. Negative feedback provides both the attenuation of the instantaneous differential response to strong stimuli and the decrease in sensitivity (to small input increments) as the background gets stronger. Adaptation, as we see it, goes beyond attenuation of response to stronger stimuli. It is the capacity of the system to modify its characteristics (e.g., gain) on a slow time scale, in response to a change in the statistical properties of the input. Thus the fundamental issue in adaptation is its time-scale dependence. It is likely that within the phototransduction cascade, adaptation occurs on a broad range of time scales ranging from seconds to minutes to perhaps days. The different Ca feedback loops (Koutalos and Yau, 1996) may correspond to different relatively short time scales (less than a minute), and this issue deserves further investigation. It is conceivable that other, yet unknown feedback mechanisms operate in rod cells on even longer time scales.

The “tunability” of signal transduction characteristics of an enzymatic cascade via concentrations of its molecular components has been the main theme of the present work. Whereas biochemical systems are often studied and discussed with the emphasis on kinetic constants and often remarkable catalytic efficiencies of their key enzymes, it is evident that on the time scale short compared with significant evolution of individual proteins, the behavior of an enzymatic system is “controlled” by the concentrations of its molecular components. The latter are the only parameters available to evolution in constructing, from nearly con-

served components, signal transduction systems functioning under diverse conditions. Thus it will be interesting to compare enzyme concentration levels between rods and cones, between different species, and ultimately between different G-protein-coupled cGMP mediated cascades (e.g., taste transduction; Kolesnikov and Margolskee, 1995).

An amusing example of this “tunability principle” is provided by the time constant of G_{α}^* , a key parameter determining the gain in the first stage of phototransduction. It is controlled by the rate of GTPase activity of G_{α}^* , which, in the preliminary version of this manuscript, entered as a kinetic parameter τ_H^{-1} . Recent work (Chen et al., 2000) has demonstrated that τ_H^{-1} is in fact regulated by the RGS9-1 (“regulator of G-protein signaling” protein) and thus can be controlled by its concentration! Because decreasing τ_H is one of the most direct ways of reducing the transduction gain, it may turn out to play a role in adaptation (perhaps in cones, where attenuation of the static response is more pronounced).

Feedback effects regulate transduction characteristics through allosteric modification of enzymatic activity. Ultimately, however, the system properties are “encoded” in total amounts of different proteins, which are determined via complex mechanisms of transcription and translation control competing with protein degradation. Is it possible that the set of enzyme concentrations is not entirely determined as a heritable property subject to selection, but is controlled at least in part by some form of intracellular feedback linking gene expression with the functional state of the cell? For example, could prolonged saturation of ROS result in changes in enzyme concentrations so as to reduce transduction gain and bring the cell out of saturation? It is not too difficult to imagine a biochemically plausible realization of such a mechanism. The result of such “functional feedback” would be self-tuning of the cascade. An example of such self-tuning has been described (Turrigiano, 1994) in a different context. This issue may be addressed through the study of genetically modified animals. For example, overexpression of GC in rods is expected to result in higher cascade gain. It may be counteracted, however, in a number of ways: e.g., reduction of the number of channels, increase in [PDE], GCAP-mediated shift in the Ca feedback gain, etc. An observation of any such compensatory change would indicate the existence of “intracellular plasticity.” Quantitative understanding of the basic enzymatic cascade opens the way to the study of potentially more complex regulatory processes underlying robust functionality.

APPENDIX A: QUANTITATIVE DESCRIPTION OF PHOTOTRANSDUCTION IN THE ROD OUTER SEGMENT

In this appendix, we review the chemical kinetic equations governing the cascade (Lamb and Pugh, 1992; Tranchina et al., 1991). The light detection

step is modeled by

$$d[\text{Rh}^*]/dt = (\sigma^2 I + \gamma_s)[\text{Rh}] - \tau_{\text{Rh}^*}^{-1}[\text{Rh}^*], \quad (33)$$

where I is the incident light intensity, σ^2 is the absorption cross section, and $[\text{Rh}]$ and $[\text{Rh}^*]$ are the concentrations of rhodopsin and metarhodopsin II, respectively. The spontaneous activation rate of Rh, $\gamma_s \approx 10^{-11} \text{ s}^{-1}$, is very small (Stryer, 1991). Though the deactivation of excited rhodopsin involves multiple steps, here we will assume that it effectively occurs in a single step with a time constant τ_{Rh^*} . This time constant is set by the activity of rhodopsin kinase and arrestin, which are modulated in turn by intracellular $[\text{Ca}]$ (Koutalos and Yau, 1996).

The encounter and interaction of excited rhodopsin with many G protein molecules causes each of them to release GDP and bind GTP to produce G α -GTP (G^*) at a rate $k_{\text{Rh}}[G]/(1 + [G]/K_{\text{Rh}})$. G α -GTP then activates cGMP phosphodiesterase (PDE) with a rate constant K_2 . The rate equation for the concentration of G α -GTP, $[G^*]$ is thus

$$d[G^*]/dt = \frac{k_{\text{Rh}}[G]}{1 + [G]/K_{\text{Rh}}}[\text{Rh}^*] - K_2[\text{PDE}][G^*]. \quad (34)$$

The kinetics of PDE* production is given by

$$d[\text{PDE}^*]/dt = K_2[\text{PDE}][G^*] - \tau_{\text{H}}^{-1}[\text{PDE}^*], \quad (35)$$

where $[\text{PDE}^*]$ is the concentration of activated PDE and τ_{H}^{-1} is the rate of hydrolysis of excited PDE-G α and the consequent inhibition of PDE activity (Stryer, 1991, 1995). The G-protein loop amplifies the changes in Rh* into the changes in the number of active phosphodiesterase molecules PDE*, given by,

$$\text{PDE}^* = \tau_{\text{H}} \frac{k_{\text{Rh}}[G]}{1 + [G]/K_{\text{Rh}}}[\text{Rh}^*]. \quad (36)$$

The static gain, $g_1 \equiv d\text{PDE}^*/d\text{Rh}^*$, is given by the prefactor of Rh* on the r.h.s. of Eq. 36,

$$g_1 = \tau_{\text{H}} \frac{k_{\text{Rh}}[G]}{1 + [G]/K_{\text{Rh}}}. \quad (37)$$

In the second stage, the activated PDE molecules (PDE*) hydrolyze cGMP in the cytoplasm. The rate of change of cGMP concentration, $[\text{cG}]$, is given by

$$d[\text{cGMP}]/dt = -k_{\text{cG}}^*[\text{PDE}^*][\text{cGMP}] - k_{\text{cG}}[\text{PDE}][\text{cGMP}] + \gamma_{\text{GC}}[\text{GC}]. \quad (38)$$

Here, $k_{\text{cG}}^*[\text{PDE}^*][\text{cGMP}]$ is the rate of hydrolysis of cGMP by PDE*, $k_{\text{cG}}[\text{PDE}][\text{cGMP}]$ is the rate of hydrolysis of cGMP by PDE, and $\gamma_{\text{GC}}[\text{GC}]$ is the rate of production of cGMP by GC. In a steady state,

$$[\text{cGMP}] = \tau_{\text{cG}} \gamma_{\text{GC}}[\text{GC}], \quad (39)$$

with the time constant

$$\tau_{\text{cG}} = (k_{\text{cG}}[\text{PDE}] + k_{\text{cG}}^*[\text{PDE}^*])^{-1}. \quad (40)$$

(The factor of 10^{-3} ratio of the catalytic rates of inhibited and uninhibited phosphodiesterase $k_{\text{cG}}/k_{\text{cG}}^*$ may alternatively be thought of as the spontaneous activation equilibrium ratio.) The rate of cGMP resynthesis γ_{GC} by GC strongly depends (Koch and Stryer, 1988) on $[\text{Ca}]$ via intermediary Ca-binding protein(s) (Gorzcyca et al., 1994; Klenchin et al., 1995), providing a handle for feedback and regulation. Note that $[\text{cGMP}]$ depends on the input light intensity via $[\text{PDE}^*]$ dependence of τ_{cG} , and the

static gain of this second transduction stage is

$$g_2 \equiv d\text{cGMP}/d\text{PDE}^* = -\tau_{\text{cG}} k_{\text{cG}}^*[\text{cGMP}]. \quad (41)$$

As we remarked in the second section for the general case, gain can be increased either at the expense of the “bandwidth” τ_{cG}^{-1} or by increasing $[\text{cGMP}]$ (through an increase in $[\text{GC}]$). Using (Stryer, 1991) $k_{\text{cG}}^* = 50 \mu\text{M}^{-1} \text{ s}^{-1}$ and $[\text{cGMP}] = 5 \mu\text{M}$, we estimate the maximal $|g_2|$ (assuming $\tau_{\text{cG}} < 1 \text{ s}$) to be ~ 250 .

Next we discuss the transduction of the cGMP messenger signal into membrane potential V . The number of open channels, Ch*, depends on $[\text{cGMP}]$ through

$$\text{Ch}^* = ([\text{cGMP}]/K_{\text{cG}})^3 \text{Ch}, \quad (42)$$

where Ch is the total number of channels and $K_{\text{cG}} \approx 12 \mu\text{M}$ is estimated from the observed fraction of open channels in the dark (i.e., $\text{Ch}^*/\text{Ch} = 0.05$ for the toad with $[\text{cGMP}] = 5 \mu\text{M}$ in the dark). It is assumed that the dynamics of channel opening and closure is fast on the scale of τ_{cG} or τ_{Rh^*} .

The simplest model for the ionic current flow in the rod cell is one in which the inner and outer segments are at the same potential and have membrane resistances R_{in} and σ_{out}^{-1} , respectively. The potential difference between the interior and exterior of the rod cell, V , is maintained by ion pumps which produce a potential-dependent current, I_p . This current has to be balanced by the leak current through the membranes, which is just $(\sigma_{\text{out}} + R_{\text{in}}^{-1})V$. This determines the voltage V to be $I_p/(\sigma_{\text{out}} + R_{\text{in}}^{-1})$. When I_p is not strongly dependent on V , to produce a strong dependence of the voltage on σ_{out} (which in turn depends on the number of open channels) and to maximize sensitivity, we need $\sigma_{\text{out}} \approx R_{\text{in}}^{-1}$. When all of the channels are closed and $\sigma_{\text{out}} = 0$, the voltage, $v = V_{\text{sat}} = I_p R_{\text{in}}$. Thus,

$$V - V_{\text{sat}} = v \times \sigma_{\text{out}} R_{\text{in}} / (1 + \sigma_{\text{out}} R_{\text{in}}), \quad (43)$$

with $v = I_p R_{\text{in}}$.

Calcium flow through the open channels I_{Ca} is proportional to Ch^* . The change in the calcium concentration with time as a result of the incident photon is given by

$$d[\text{Ca}]/dt = I_{\text{Ca}} - \tau_{\text{Ca}}^{-1}[\text{Ca}], \quad (44)$$

where τ_{Ca} is the calcium time constant. The terms involving the calcium buffers have not been explicitly included in the equation. The Ca/Na/K exchanger pumps Ca out at a high rate (Gray-Keller and Detwiler, 1994), which sets the time constant $\tau_{\text{Ca}} \approx 10^{-2} \text{ s}$, so that on the time scale of the response, $[\text{Ca}]$ concentration closely follows the number of open channels. (It is known that only a small fraction (0.04) of Ca in ROS is free (Koutalos and Yau, 1996; Gray-Keller and Detwiler, 1994); the rest is bound. It is reasonable to assume that the dynamics of “buffered” Ca is slow (on the scale of τ_{Rh^*}) and is neglected here.) However, the presence of calcium buffers may slow the response. The calcium current can be related to the concentration of cGMP through

$$I_{\text{Ca}} = \sigma[\text{Ca}]_{\text{ext}} \frac{[\text{cGMP}]^3}{K_{\text{cG}}^3}, \quad (45)$$

where $\sigma[\text{Ca}]_{\text{ext}} = 1.5 \times 10^3 \mu\text{M/s}$ and $K_{\text{cG}} = 12 \mu\text{M}$. The resulting change in calcium concentration affects the resynthesis of cGMP by GC and can be modeled by a functional dependence of γ_{GC} on the calcium concentration as

$$\gamma_{\text{GC}} = \frac{\gamma_{\text{GC}}^0}{1 + ([\text{Ca}]/K_{\text{D}})^2}, \quad (46)$$

From this one can compute the effective gain for the second stage with calcium feedback, which is just given by Eq. 22 with

$$g_c = 3[\overline{\text{Ca}}]/[\overline{\text{cGMP}}],$$

$$g_{xc} = 2 \frac{[\overline{\text{cGMP}}]}{[\overline{\text{Ca}}]} \frac{([\overline{\text{Ca}}]/K_D)^2}{1 + ([\overline{\text{Ca}}]/K_D)^2},$$

$\tau = \tau_{cG}$ and $\tau_c = \tau_{ca}$. Thus, the zero frequency gain is given by Eq. 23 with

$$Y = 1 + 6 \frac{[\overline{\text{Ca}}]^2}{K_D^2 + [\overline{\text{Ca}}]^2}. \quad (47)$$

This gain reduction factor in the dark is close to 7. Depending on the relative values of τ_{cG} and τ_{fdbk} , one could get different scenarios described in Fig. 4. We have already mentioned the $[\text{Ca}]$ concentration dependence of the GC rate (Koch and Stryer, 1988) and of τ_{Rh} , which provide the feedback regulation (Koutalos and Yau, 1996). The gain factor Y can be tuned by adjusting the concentration of GCAP proteins or the number of exchangers, and the feedback time constant, τ_{fdbk} , can be changed by adjusting the GCAP concentration, as shown in the next appendix. Thus, again, the parameters of the cascade can be tuned by changing the concentrations of various enzymes.

APPENDIX B: CALCIUM FEEDBACK

In this appendix we consider in more detail a minimal model of calcium feedback (Koutalos and Yau, 1996) to elucidate Eq. 46 and to demonstrate again how the parameters of the cascade (the gain factor and time constant) can be controlled by relative concentrations of various enzymes. This is true generically and is independent of the details of our model. Let us assume that Ca enters the cell at a rate I_{ca} and is pumped out at a rate $\gamma_{ex}Ex$ proportional to the number of exchangers. It is taken up in 2:1 stoichiometry by GC activating protein (GCAP). For the sake of simplicity we omit other possible Ca buffers. The rate equation governing the calcium dynamics can be written as

$$\frac{d[\text{Ca}]}{dt} = -\gamma_{ex}Ex[\text{Ca}] + I_{ca} - (k_{\text{gcapL}}[\text{Ca}]^2[\text{GCAP}] - k'_{\text{gcapL}}[\text{GCAP}_{Ca}]), \quad (48)$$

where I_{ca} is the calcium current given by Eq. 45, $[\text{GCAP}]$ is the concentration of calcium-binding GCAP protein, $[\text{GCAP}_{Ca}]$ is that of the calcium-GCAP complex, and k_{gcap} and k'_{gcap} are rate constants. GCAP protein binds to and activates GC but GCAP_{Ca} complex does not. The dynamics of GC activation can be modeled by

$$\frac{d[\text{GC}^*]}{dt} = k_{\text{GC}}[\text{GCAP}][\text{GC}] - k'_{\text{GC}}[\text{GC}^*],$$

with only $[\text{GC}^*]$ responsible for the production of cyclic GMP. From these kinetic equations, one obtains

$$K_D \approx k'_{\text{GCAP}}k_{\text{GC}}[\text{GCAP}_{\text{tot}}]/(k_{\text{GCAP}}k'_{\text{GC}}) \quad (49)$$

(assuming, for simplicity, $k'_{\text{GCAP}} \ll k_{\text{GCAP}}[\text{Ca}]^2$) and hence is tunable by alteration of the concentration of the GCAP proteins. Similarly, we find that τ_{ca} can be varied independently of K_D , through the number of exchangers, because $\tau_{ca} \sim Ex$. We also see that the gain factor Y in Eq. 47 can be tuned both by changing K_D through $[\text{GCAP}_{\text{tot}}]$ and by changing $[\overline{\text{Ca}}]$ via τ_{ca} , controlled by the number of exchangers Ex . The characteristic time of the feedback is dominated by the slowest time scale, which, since, according to Rispoli et al. (1993), τ_{ca} is fast, must be the response time of

$[\text{GC}^*]$, and thus $\tau_{fdbk} = k_{\text{GC}}[\overline{\text{GCAP}}] + k_{\text{GC}}$, which can be tuned by changing the total concentration of GCAP alone. Thus, the feedback time scale and the gain factor can be independently tuned.

APPENDIX C: BIOCHEMICAL PARAMETERS

The table below contains the values of the various parameters defined in the text. Some of the parameters (e.g., those in Eq. 48) are not known and are not included here.

τ_{H}^{-1}	k_1	K_2	k_{cG}^*	k_{cG}	$\gamma_{\text{GC}}^0[\text{GC}]$	
10/2	10 ³ /s	1 μm ² /s	50 μM ⁻¹ /s	0.05 μM ⁻¹ /s	60 μM/s	
$[\text{cG}]$	$[\text{Rh}]$	$[\text{G}]$	$[\text{PDE}]$	K_D	$\sigma[\text{Ca}]_{\text{ext}}$	K_{cG}
5 μM	5000 μM	500 μM	20 μM	0.2 μM	1.5 × 10 ³ μM/s	12 μM

APPENDIX D: INFORMATION THEORY ON THE OPTIMAL INPUT/OUTPUT RELATION

Let input $y \geq 0$ occur with probability $P(y)$ and let the range of the output be restricted to $0 \leq z \leq z_M$, e.g., because the number of vesicles that may undergo exocytosis in time τ is finite. If the noise of transduction is small compared with the amplified input noise, the mutual information is

$$M_{z|y} \approx \int dy P(y) \ln \left[\frac{\sqrt{N_z(f(y))G^{-2}(y) + N_y(y)P(y)}}{\sqrt{N_z(f(y))}} \right]^{-1}, \quad (50)$$

where $G(y) = dz/dy = f'(y)$ is the differential gain, which may be chosen so as to maximize $M_{z|y}$. (We assume a Gaussian distribution of x and y fluctuations.) The meaning of this is made clear by considering the limit when the amplified input noise $N_y G^2$ is much larger than the readout noise N_z : in that case the transduction is perfect and $M_{y|x}$ is maximized (equal to the entropy or information content of the input corrected for the input noise). As $N_y G^2/N_z$ decreases, so does the mutual information, indicating the loss in information transfer capacity. However, because the gain cannot be set arbitrarily large because of the dynamic range considerations, there is a nontrivial trade-off, and the optimal solution can be shown to satisfy

$$\frac{\sqrt{N_y(y)} dz}{\sqrt{N_z(f(y))} dy} + \left(\frac{\sqrt{N_y(y)} dz}{\sqrt{N_z(f(y))} dy} \right)^3 = cP(y) \sqrt{N_y(y)}, \quad (51)$$

with the arbitrary constant c fixed by imposing the constraint of the output dynamic range $\int dy dz/dy = z_M$. Equation 51 is simplified if z , y are measured in their natural units, the r.m.s. fluctuations $\sqrt{N_{z,y}}$: i.e., $du = dy/\sqrt{N_y(y)}$ and $dv = dz/\sqrt{N_z(z)}$, in terms of which $dv/du + (dv/du)^3 = c\tilde{P}(v)$. These u , v variables effectively label the “distinguishable” input and output states. If the initial distribution were uniform over a finite range u_M which equals the output range $v(z_M)$, i.e., if the number of distinguishable input and output states were equal, then $dv/du = 1$. The optimal transduction would just map the “distinguishable states” onto each other.

In general, when the input and output dynamic ranges—in the sense of the number of “distinguishable” states—do not agree, the available resolution of the transduction process is allocated in a nontrivial manner, which depends on input statistics $P(y)$. Two distinct regimes are apparent: 1) when the effective range of inputs is smaller than the output dynamic range and 2) when the effective range of inputs is large.

In the first regime, the gain setting is high, so that $N_y G^2 > N_z$ and all of the input fluctuations are well resolved. In the context of phototransduction, this regime corresponds to low light (scotopic) conditions, where the number of absorbed photons per rod per second is not greater than ~ 10 , which, accounting for the photon shot noise, corresponds to only $\sqrt{10}$ distinguishable states—a modest dynamic range. (Note that the scotopic range extends downward to photon fluxes nearly 10^{-4} times smaller

(Shapley, 1989); however, the response to such low light levels is a network and not a single rod cell property. Perception under low light conditions appears to average the response of $\sim 10^3$ rods.) It is well known (Baylor et al., 1974) that rods respond to a single-photon absorption event and absorb nearly all incident photons and thus fully resolve input fluctuations.

The second, wide-input dynamic range regime requires a lower setting of the gain $N_y G^2 < N_z$ and hence does not resolve input fluctuations. In this limit, Eq. 51 reduces to

$$\frac{\sqrt{N_y(y)}}{\sqrt{N_z(f(y))}} \frac{dz}{dy} = cP(y) \sqrt{N_y(y)}. \quad (52)$$

This equation just says that the probability distribution of v defined previously is uniform. This is used in the text.

Finally we make a note on information transfer for the case of the time-dependent signals in the nonlinear model. Let the system respond to a change in a signal in a typical time, τ_{nl} . For very small changes from a certain steady state, τ_{nl} is just τ in this steady state, as defined in Eq. 6. The total information transfer is the sum of the information transferred over intervals of length τ_{nl} or larger. In principle, one could use the argument about matching distinguishable states of the input and output to maximize information transfer over that period (given by Eq. 50). The information transfer rate calculated would be the channel capacity (Cover and Thomas, 1989). In a cascade, this capacity is limited by the stage with the minimal information transfer rate. For phototransduction the bottleneck is at the vesicle release stage. Our estimate shows this to result in a bit rate on the order of 5 bits/s.

We thank W. Denk, S. Leibler, R. Sarpeshkar, and E. Siggia for useful discussions. PBD thanks Bell Laboratories for its hospitality and acknowledges support from the National Institutes of Health (grant EY-02048).

REFERENCES

- Alberts, B., D. Bray, J. Lewis, M. Raff, K. Roberts, and J. Watson. 1994. *Molecular Biology of the Cell*. Garland, New York.
- Alon, U., M. Surette, N. Barkai, and S. Leibler. 1999. Robustness in bacterial chemotaxis. *Nature*. 397:168–171.
- Atick, J. J. 1992. Could information theory provide an ecological theory of sensory processing? In *Princeton Lectures on Biophysics*. W. Bialek, editor. World Scientific, Singapore.
- Barkai, N., and S. Leibler. 1997. Robustness in simple biochemical networks. *Nature*. 387:913–917.
- Baylor, D. A. 1996. How photons start vision. *Proc. Natl. Acad. Sci. USA*. 93:560–565.
- Baylor, D. A., A. L. Hodgkin, and T. D. Lamb. 1974. The electrical response of turtle cones to flashes and steps of light. *J. Physiol. (Lond.)*. 242:685–727.
- Berg, H. C. 1990. Bacterial microprocessing. *Cold Spring Harb. Symp. Quant. Biol.* 55:539–545.
- Bodoia, R. D., and P. B. Detwiler. 1985. Patch clamp recording of the light sensitive dark noise in retinal rods from lizard and frog. *J. Physiol. (Lond.)*. 367:183–216.
- Bownds, M. D., and V. Y. Arshavsky. 1995. What are the mechanisms of photoreceptor adaptation? *Behav. Brain Sci.* 18:415–424.
- Bray, D. 1995. Protein molecules as computational elements in living cells. *Nature*. 376:307–312.
- Chen, C.-K., M. E. Burns, W. He, T. G. Wensel, D. A. Baylor, and M. I. Simon. 2000. Slowed recovery of rod photoreponse in mice lacking the GTPase accelerating protein RGS9-1. *Nature*. 403:557–560.
- Chock, P. B., and E. R. Stadtman. 1977. Superiority of interconvertible enzyme cascades in metabolic regulation: analysis of multicyclic systems. *Proc. Natl. Acad. Sci. USA*. 74:2766–2770.
- Cover, T., and J. Thomas. 1989. *Elements of Information Theory*. Wiley and Sons, New York.
- Dowling, J. E. 1987. *The Retina: An Approachable Part of the Brain*. Belknap/Harvard University Press, Cambridge, MA.
- Fawzi, A. B., and J. K. Northrup. 1990. Guanine nucleotide binding characteristics of transducin: essential role of rhodopsin for rapid exchange of guanine nucleotides. *Biochemistry*. 19:3804–3812.
- Gerhart, J., and M. Kirschner. 1997. *Cells, Embryos, and Evolution*. Blackwell Science, Cambridge, MA.
- Gold, G. H., and E. N. Pugh, Jr. 1997. The nose leads the eye. *Nature*. 385:677.
- Gorczyca, W. A., M. P. Gray-Keller, P. B. Detwiler, and K. Palczewski. 1994. Purification and physiological identification of a guanylate cyclase activating protein from retinal rods. *Proc. Natl. Acad. Sci. USA*. 91:4014–4018.
- Gray-Keller, M. P., W. Denk, B. Shraiman, and P. Detwiler. 1999. Spatial spread of second messenger signals in rod photoreceptor outer segments. *J. Physiol. (Lond.)*. 519:679–692.
- Gray-Keller, M. P., and P. B. Detwiler. 1994. The Ca feedback signal in the phototransduction cascade of vertebrate rods. *Neuron*. 13:849–861.
- He, W., C. W. Cowan, and T. G. Wensel. 1998. RGS9, a GTPase accelerator for phototransduction. *Neuron*. 20:95–102.
- Klenchin, V. A., P. D. Calvert, and M. D. Bownds. 1995. Inhibition of rhodopsin kinase by recoverin—further evidence for negative feedback system in phototransduction. *J. Biol. Chem.* 270:16147–16152.
- Koch, K. W., and L. Stryer. 1988. Highly cooperative feedback control of retinal rod guanylate cyclase by calcium ions. *Nature*. 334:64–66.
- Kolesnikov, S. V., and R. F. Margolskee. 1995. A cyclic nucleotide suppressible conductance activated by transducin in taste cells. *Nature*. 376:85–87.
- Koshland, D. E., Jr. 1980. Biochemistry of sensing and adaptation. *Trends Biochem. Sci.* 5:297.
- Koshland, D. E., Jr., A. Goldbeter, and J. B. Stock. 1978. Amplification and adaptation in regulatory and sensory systems. *Science*. 217:220.
- Koutalos, Y., and K.-W. Yau. 1996. Regulation of sensitivity in vertebrate rod photoreceptors by calcium. *Trends Neurosci.* 19:73–81.
- Lamb, T. D., and E. N. Pugh, Jr. 1992. A quantitative account of the activation steps involved in phototransduction in amphibian photoreceptors. *J. Physiol. (Lond.)*. 449:710–758.
- Laughlin, S. B. 1981. A simple coding procedure enhances neuron's information capacity. *Z. Naturforsch.* 36c:910–912.
- Lauffenburger, D. A., and J. J. Linderman. 1993. *Receptors*. Oxford University Press, Oxford.
- Naka, K.-I., M.-O. Itoh, and R. L. Chappell. 1987. Dynamics of turtle cones. *J. Gen. Physiol.* 89:321–337.
- Nikonov, S., N. Engheta, and E. N. Pugh, Jr. 1998. The kinetics of recovery of dark-adapted salamander rod photoreponse. *J. Gen. Physiol.* 111:7–37.
- Normann, R. A., and I. Perlman. 1979. The effects of background illumination on the photoreponses of red and green cones. *J. Physiol. (Lond.)*. 286:491–501.
- Pepperberg, D. R., M. C. Cornwall, M. Kahlert, K. P. Hoffmann, J. Jin, G. J. Jones, and H. Ripps. 1992. Light-dependent delay in the falling phase of retinal rod photoreponse. *Vis. Neurosci.* 8:9–18.
- Ptashne, M. 1992. *Genetic Switch: Phage Lambda and Higher Organisms*, 2nd Ed. (rev. printing 1998). Blackwell Science, Cambridge, MA.
- Reed, R. R. 1990. How does the nose know? *Cell*. 60:1–2.
- Rieke, F., and D. Baylor. 1996. Molecular origin of continuous dark noise in rod photoreponses. *Biophys. J.* 71:2553–2572.
- Rieke, F., and D. Baylor. 1998. Origin of reproducibility in the responses of single rods to photons. *Biophys. J.* 75:1836–1857.
- Rieke, F., and E. Schwartz. 1994. A cGMP gate current can control exocytosis at cone synapse. *Neuron*. 13:863–873.
- Rieke, F., and E. Schwartz. 1996. Asynchronous transmitter release: control of exocytosis and endocytosis at the salamander rod synapse. *J. Physiol. (Lond.)*. 493:1–8.

- Rispoli, G., W. A. Sarher, and P. B. Detwiler. 1993. Visual transduction in dialyzed detached rod outer segments from lizard retina. *J. Physiol. (Lond.)* 465:513–537.
- Shapley, R. M., and C. Enroth-Cugell. 1989. Visual adaptation and retinal gain controls. In *Progress in Retinal Research*, Vol. 3. N. Osborne and G. Chader, editors. Pergamon Press, London. 263–346.
- Simon, M. I., M. P. Strathman, and N. Gautam. 1991. Diversity of G-proteins in signal transduction. *Science*. 252:802–808.
- Stadtman, E. R., and P. B. Chock. 1977. *Proc. Natl. Acad. Sci. USA*. 74:2761–2765.
- Stryer, L. 1991. Visual excitation and recovery. *J. Biol. Chem.* 266: 10711–10714.
- Stryer, L. 1995. *Biochemistry*. Freeman, New York.
- Tranchina, D., J. Sneyd, and I. D. Cadenas. 1991. Light adaptation in turtle cones. *Biophys. J.* 60:217–237.
- Turrigiano, G., L. F. Abbott, and E. Marder. 1994. Activity-dependent changes in the intrinsic properties of cultured neurons. *Science*. 264: 974–977.
- Wray, G. A. 1998. Promoter logic. *Science*. 279:1871–1872.